Magnetisation measurements of the synthetic olivine single crystals A_2SiO_4 with A=Mn, Fe or Co

1989 J. Phys.: Condens. Matter 1 4955

(http://iopscience.iop.org/0953-8984/1/30/009)

J. Phys.: Condens. Matter **1** (1989) 4955–4970. Printed in the UK

Magnetisation measurements of the synthetic olivine single crystals A_2SiO_4 with A = Mn, Fe or Co

O Ballet†‡, H Fuess†, K Wacker§, E Untersteller§, W Treutmann§, E Hellner§ and S Hosoya¶

† Institut für Kristallographie und Mineralogie, Senckenberganlage 30, D-6000 Frankfurt, Federal Republic of Germany

§ Institut für Kristallographie und Mineralogie, Lahnberge, D-3550 Marburg, Federal Republic of Germany

¶ Institute for Materials Research, Tohoku University, Katahira, Sendai 980, Japan

Received 8 June 1988, in final form 23 November 1988

Abstract. Magnetisation measurements of three synthetic single-crystals A_2SiO_4 of the olivine family are presented (A = Mn, Fe and Co). All three compounds order antiferromagnetically in the range 45–65 K. For A = Mn, weak ferromagnetism is present. For A = Fe and Co, the magnetisation is strongly anisotropic. A model is proposed, which extends existing published explanations of the magnetic structures. The magnetic cations are represented by spin Hamiltonians, and their interactions by mean fields. Analytical relationships are derived between Curie temperatures, Curie constants and Néel temperatures on the one hand, and spin Hamiltonian parameters on the other. From the latter parameters the maximum possible information on orbital levels is derived. This is enough to calculate magnetic entropies in good agreement with published data, together with specific heat measurements, and to point out the limits of validity of the linearisation processes that are necessary to obtain usable analytical relations between experimental and atomic parameters. Below T_N, the susceptibilities are analysed using the conclusions of previous magnetic structure studies, especially those concerning the role of competing exchanges, single-ion anisotropies, and symmetry requirements.

1. Introduction

The magnetic susceptibility of a powder of Co_2SiO_4 has been measured as a function of temperature by Nomura *et al* (1964), and that of powders of Mn_2SiO_4 and Fe_2SiO_4 by Santoro *et al* (1966). In all three olivines a critical temperature was found above which the susceptibility is paramagnetic. These authors also observed the powder neutron diffraction pattern at 4.2 K and 300 K in all three samples, and in addition at 58 K and 77 K in Fe_2SiO_4. The magnetic structure at 4.2 K was found to be antiferromagnetic in all cases, with the magnetic cell equal to the crystallographic cell. The decrease in the susceptibility of Co_2SiO_4 below the transition temperature was not surprising in view of the antiferromagnetism of the silicate. As for the other two powders, the evolution of their reciprocal susceptibilities with decreasing temperature was considered as 'almost identical'.

‡ Deceased.

0953-8984/89/304955 + 16 $02.50

Although the curves show many features, a maximum seen well below the ordering transition was interpreted as being due to a second transition. This was related to the canting of the magnetic moments of the 4a sites observed at 4.2 K in these two silicates but not in Co_2SiO_4. Since for Fe_2SiO_4 the pattern at 58 K seemed to show no canting, a magnetic transition between a collinear structure and a canted structure was naturally put forward.

Takei and Hosoya (1982) succeeded in growing pure single crystals of these compounds. Lottermoser *et al* (1986) and Lottermoser and Fuess (1988) followed the neutron reflections of these crystals over a range of temperatures below the Néel temperature (T_N), and found that canting exists in all three silicates. However, the thermal behaviour of the canting is very different for the three crystals. In Mn_2SiO_4, the canting is very weak down to a temperature where it increases rapidly with decreasing temperature. In contrast, at decreasing temperature the canting increases monotonically in Fe_2SiO_4 and remains constant in Co_2SiO_4. Ballet and Fuess (1989) interpreted the magnetic structures and their thermal evolutions by considering both exchange interactions and single-ion anisotropies, and in making full use of the symmetry relationships between the magnetic sites.

The present paper reports a magnetometer study of these crystals. The susceptibility is clearly anisotropic for Fe_2SiO_4 and Co_2SiO_4. As a function of temperature, the susceptibility curves contrast considerably with one another on one hand, and from the powder susceptibility on the other. We propose explanations for the main features of these curves by extending the interpretation by Ballet and Fuess (1989) of the underlying magnetic structures to the effect on them of an applied magnetic field. Analytical relations are established between the paramagnetic Curie temperatures (θ_α) and Curie constants (C_α) along the three axes, as well as the ordering temperature (T_N) and the exchange and anisotropy parameters. This analytical discussion relies on the assumption that the magnetic cations can be described by spin Hamiltonians, and their interactions by the mean-field scheme.

2. Materials and experiment

2.1. Crystal growth

Olivine minerals (A_2SiO_4) occur in nature only in the form of solid solutions. Synthetic end-member olivines can be grown in the laboratory. Takei and Hosoya (1982) pointed out that the choice of the growth method plays a decisive role in the quality of the crystals. Large, high-quality olivine single crystals of Mn_2SiO_4 (tephroite) have been grown by the Czochralski method, and Fe_2SiO_4 (fayalite) and Co_2SiO_4 by the floating-zone method in a controlled atmosphere using focused radiation heating (Takei *et al* 1984). The typical crystal size was 7 mm in diameter and 70 mm in length. The growth directions of the crystals on which we performed our experiments were [001] for tephroite and fayalite and [100] for Co olivine. Crystallographically oriented rectangular samples were cut out of the middle of these crystals. Quality and orientation were checked by x-ray and neutron diffraction.

2.2. Experiment

The magnetic measurements were carried out with a vibrating-sample magnetometer (VSM model: PAR 159) (Foner 1959). The cryogenic system (Dewar assembly: model

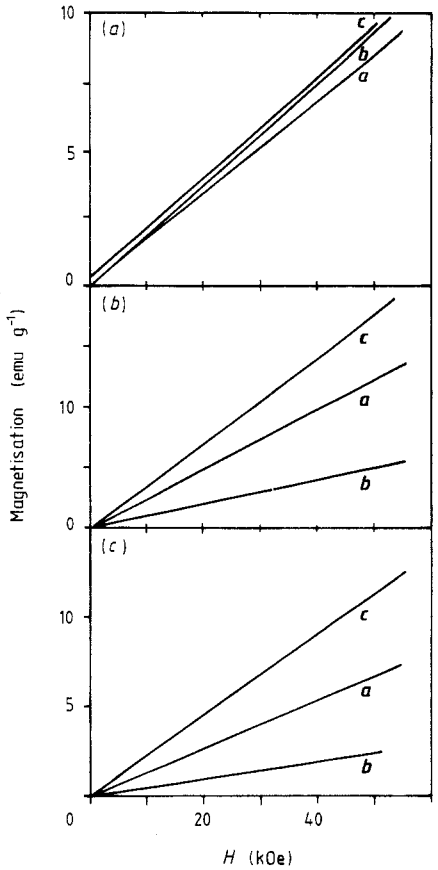

Figure 1. Magnetisation against applied field at $T = 4.2$ K for (*a*) Mn_2SiO_4; (*b*) Fe_2SiO_4; (*c*) Co_2SiO_4.

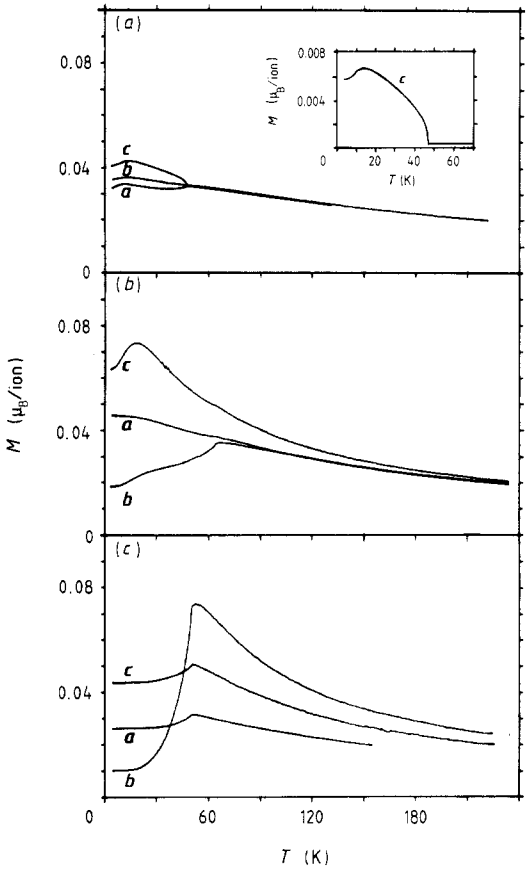

Figure 2. Magnetisation against temperature in a field of 10 kOe for (*a*) Mn_2SiO_4; (*b*) Fe_2SiO_4; (*c*) Co_2SiO_4. Inset, magnetisation against temperature along the *c* axis in Mn_2SiO_4 in zero field.

159, Janis Research Company) performs two functions: it cools the superconducting magnet (split coil), and cools the sample to the required temperature, which is regulated by a cryogenic temperature controller (PAR 152). For monitoring the sample temperature, a calibrated carbon glass resistor (CGR 1-1000, Lake Shore Cryotronics Inc.) is located in the rod itself immediately adjacent to the sample. The influence of strong magnetic fields on the nominal temperature is very small (0.1 K under 50 kOe).

The magnetometer itself was calibrated by using a cylindrical sample of high-purity nickel supplied by PAR. The magnetometer was fully monitored, and the data processed by home-made computer programs. A goniometer allowed the crystal to rotate around the vibrating axis in the applied magnetic field. The magnetisation was measured for our three crystals along each of the three crystallographic axes ***a***, ***b*** and ***c***. The alignment was obtained within 2° by looking for the extremum effect.

2.3. Results

Magnetisation curves $M(H)$ were obtained for fields up to 50 kOe at various temperatures (figure 1); they are linear. Some measurements had been made previously by

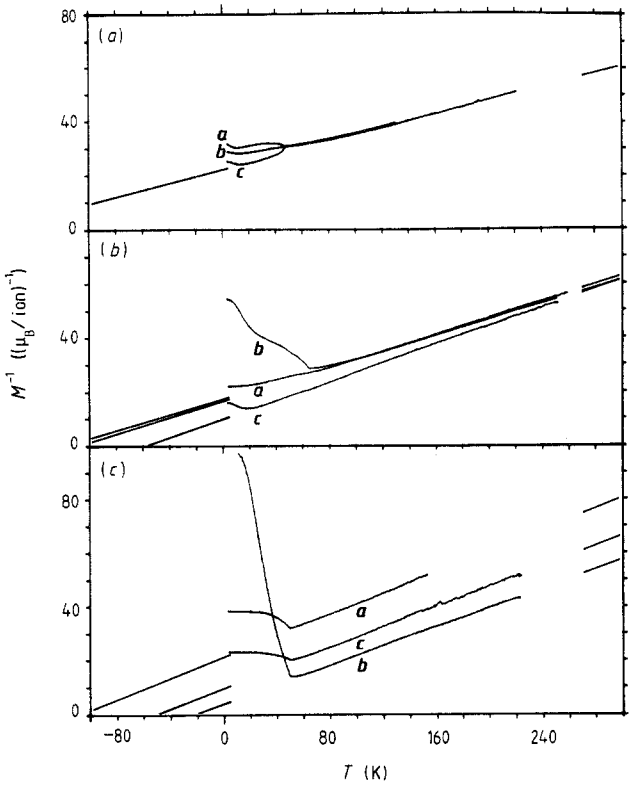

Figure 3. Inverse magnetisation against temperature in a field of 10 kOe for (*a*) Mn_2SiO_4; (*b*) Fe_2SiO_4; (*c*) Co_2SiO_4. Above T_N, the curves are fairly well fitted by straight lines, parts of which are shown above 260 K and below 5 K.

Müller *et al* (1982) on Fe_2SiO_4 crystals up to 150 kOe. No departure from linearity could be seen in this range at 35 K, whereas at 4.2 K an upward curvature appeared above 50 kOe. The magnetisation $M(T)$ at 10 kOe was followed between 4.2 K and 250 K (figure 2). Because of the linearity of $M(H)$ they also represent the initial susceptibility curves $\chi(T)$, except for Mn_2SiO_4 where a remnant magnetisation is observed along the *c*-axis. All three crystals show a critical temperature T_N which marks a drastic change in the temperature behaviour of their magnetic susceptibility. Above T_N, the inverse susceptibilities (figure 3) are linear in temperature, in agreement with the Curie law for paramagnets. Below T_N, decreasing temperature results in susceptibility variations that are highly dependent on the crystal and on the direction. In Fe_2SiO_4 and Co_2SiO_4, a decrease in susceptibility below T_N is seen along the *b*-axis, indicating antiferromagnetic ordering along this axis, in agreement with the neutron results. In Mn_2SiO_4, no decrease in susceptibility is observed at low temperature, but the weakness of the magnetisation (0.04 μ_B per ion) indicates that this is also an antiferromagnet. The weak remnant magnetisation (0.006 μ_B per ion) in the *c*-direction indicates weak ferromagnetism.

3. Theory

Our starting point will be a description of the energy of the magnetic system under an

Table 1. Magnetic modes that are invariant under one of the magnetic groups compatible with magnetic ordering of both 4a and 4c sites in Pnma.

	Γ_{+++}	Γ_{--+}	Γ_{-+-}	Γ_{+--}
4a	$A_1{}^a G_1{}^b C_1{}^c$	$G_1{}^a A_1{}^b F_1{}^c$	$F_1{}^a C_1{}^b G_1{}^c$	$C_1{}^a F_1{}^b A_1{}^c$
4c	$G_5{}^b$	$G_5{}^a \quad F_5{}^c$	$F_5{}^a \quad G_5{}^c$	$F_5{}^b$

external field H, by:

$$-(\tfrac{1}{2})\sum_{ij\alpha} J_{ij} Z_{ij} S_i{}^\alpha S_j{}^\alpha - (\tfrac{1}{2})\sum_{i\alpha\beta} A_i{}^{\alpha\beta} S_i{}^\alpha S_i{}^\beta - (\tfrac{1}{2})\sum_{ij\alpha\beta} \mu_i{}^\alpha T_{ij}{}^{\alpha\beta} \mu_j{}^\beta - \sum_{i\alpha} H^\alpha \mu_i{}^\alpha. \tag{3.1}$$

The summations are over the eight magnetic sites of a cell, and the three directions parallel to the crystallographic axes. $S_i{}^\alpha$ is the component along $\boldsymbol{\alpha}$ of the spin at site i. $\mu_i{}^\alpha$ is the magnetic moment along $\boldsymbol{\alpha}$ at site i. This is $\Sigma_\beta g_i{}^{\alpha\beta} S_i{}^\beta \mu_B$. The tensor $\mathbf{g}_i$ is the Landé factor of the ion at site i. μ_B is the Bohr magneton. We assume, therefore, that the system is made up of ions that can be described by spin Hamiltonians. The four contributions to the Hamiltonian (3.1) are successively exchange interactions, single-ion anisotropies, magnetic interactions between the magnetic moments and magnetic couplings with the applied field.

3.1. The mean-field approximation

At non-zero temperature, the stable configuration under an applied field or not, requires finding the minimum of the free energy $E - T \times S$. A classical approximation is a decoupling of the problem by considering each site as submitted to the influence of the other sites, but with no feedback interaction from this site to them. That is, no correlations of the spin fluctuations are taken into account. Then there exists a set of equations

$$\langle S_i{}^\alpha \rangle_T = f_i{}^\alpha (T, \{\langle S_j{}^\beta \rangle_T\}) \tag{3.2}$$

whose unknown is the set $\{\langle S_j^\beta \rangle_T\}$. The functions f_i^α represent Boltzmann averages of S_i^α over the energy levels of the spins i whose Hamiltonian is

$$-\sum_{j\alpha\beta} N_{ij}{}^{\alpha\beta} \langle S_j{}^\beta \rangle_T S_i{}^\alpha - (\tfrac{1}{2})\sum_{\alpha\beta} A_i{}^{\alpha\beta} S_i{}^\alpha S_i{}^\beta - \mu_B \sum_{\alpha\beta} H^\alpha g_i{}^{\alpha\beta} S_i{}^\beta \tag{3.3}$$

where $N_{ij}{}^{\alpha\beta} = J_{ij} z_{ij} \delta_{\alpha\beta} + \Sigma_{\gamma\alpha} g_i{}^{\gamma\alpha} T_{ij}{}^{\gamma\delta} g_j{}^{\delta\beta}$.

3.2. Magnetic symmetry groups

We use the conclusions of Ballet and Fuess (1989) concerning the constraints borne by the olivine crystallographic structure on the magnetic sites 4a and 4c. The spin modes or magnetic moment modes $A_1{}^\alpha$, $C_1{}^\alpha$, $G_1{}^\alpha$, $F_1{}^\alpha$ are defined on the four 4a sites as the four possible configurations affording equal lengths of the spins or of the magnetic moments along the $\boldsymbol{\alpha}$-direction (Bertaut 1963). The last one is ferromagnetic, while the others are antiferromagnetic. $\mathbf{A}_1$, $\mathbf{C}_1$ and $\mathbf{G}_1$ correspond to spin directions $+--+$, $+-+-$ and $++--$ on the ions 1, 2, 3 and 4, respectively. Ion 2 (or 4) is deduced from ion 1 (or 3) by the twofold screw rotation 2_{1b}. Similarly, $\mathbf{G}_5$ and $\mathbf{F}_5$ are defined on the 4c sites. Table 1 shows the four sets of modes that can coexist in the ordered phase when no field is applied. Each set corresponds to a different group of magnetic symmetry operations compatible with the group of the crystallographic symmetry operations. The magnetic

structures of Fe_2SiO_4 and Co_2SiO_4 belong to the Γ_{+++} group, and that of Mn_2SiO_4 to Γ_{--+}. Under a magnetic field applied along the $\boldsymbol{\alpha}$-axis, the modes of the group to which the modes F^α belong are induced. The crystallographic symmetry yields relations among the parameters that appear in the Hamiltonians; among the exchange parameters, for instance, these are $J_{38} = J_{15}$. By neglecting the indirect exchanges occurring via two oxygens with respect to those occurring via one oxygen and the direct exchanges, one is left with four parameters: J_{12} (4a–4a interactions), J_{15} and J_{35} (4a–4c) and J_{57} (4c–4c). Among the anisotropy and Landé tensors, these relations are, for instance, ${A_2}^{ab} = -{A_1}^{ab}$ and ${g_2}^{ab} = -{g_1}^{ab}$, so that only $\mathbf{A}_1$, $\mathbf{A}_5$, $\mathbf{g}_1$ and $\mathbf{g}_5$ are required. To make full use of these relationships, it is interesting to write the Hamiltonian (3.3) on the basis of the spin modes. A table representing the tensor $\mathbf{J}'$ defined by $J'_{ij} = J_{ij}Z_{ij}$ on this basis is given in Ballet and Fuess (1989). The elements of the tensors $\mathbf{A}_i$ connect only those modes that correspond to the same class of sites (4a for $i = 1$, 4c for $i = 5$) and belong, as they should, to the same magnetic group. Then, the corresponding element is merely ${A_i}^{\alpha\beta}$, whatever the two modes, where $\boldsymbol{\alpha}$ and $\boldsymbol{\beta}$ are the directions of these modes. The mirror planes perpendicular to the $\boldsymbol{b}$-axis and containing the 4c sites, constrain a principal axis to be along $\boldsymbol{b}$, i.e., ${A_5}^{ab} = 0 = {A_5}^{bc}$, and the same for $\mathbf{g}_5$. We call ${U_{mn}}^{\alpha\beta}(\Gamma)$ the elements of the magnetic dipolar interaction tensor $\mathbf{T}$ on the basis of the magnetic moment modes; m and n are 1 or 5 according to the class of sites to which the modes belong. For a given set mn, ${U_{mn}}^{\alpha\beta}(\Gamma)$ depends on the magnetic group Γ under consideration. Here again, it is verified that no elements connect the modes that do not belong to the same group. Within a given magnetic group, the non-zero elements are the following: ${U_{11}}^{\alpha\alpha} = {T_{11}}^{\alpha\alpha} + {T_{12}}^{\alpha\alpha} + {T_{13}}^{\alpha\alpha} + {T_{14}}^{\alpha\alpha}$ and ${U_{55}}^{\alpha\alpha} = {T_{55}}^{\alpha\alpha} + {T_{56}}^{\alpha\alpha} + {T_{57}}^{\alpha\alpha} + {T_{58}}^{\alpha\alpha}$, where the signs are the same as in the definition of the mode of the group that exists in the $\boldsymbol{\alpha}$-direction. ${U_{55}}^{\alpha\beta} = {T_{56}}^{\alpha\beta}$ if $\alpha \neq \beta$. ${U_{15}}^{\alpha\beta} = 2({T_{15}}^{\alpha\beta} + {T_{17}}^{\alpha\beta})$ with + (or −) if the 4c mode is ${F_5}^\beta$ (or ${G_5}^\beta$), whatever the 4a mode. The tensor $\mathbf{N}$ itself is split into subtensors $\{{N_{mn}}^{\alpha\beta}(\Gamma)\}$, one for each magnetic group.

4. Discussion

4.1. Paramagnetic susceptibility

When the temperature k_BT is much higher than the higher energy level of the Hamiltonians (3.3), the functions ${f_i}^\alpha$ appearing in (3.2) can be made linear in the arguments of the Boltzmann factors (note that $\mu_B H/k_B$ is 1 K when $H = 15$ kOe). Assuming that this condition is fulfilled, at least above 100 K, we have calculated the spin component along the $\boldsymbol{\beta}$ crystallographic axis, which is induced on the site i by a field applied along the $\boldsymbol{\alpha}$ crystallographic axis:

$$\langle {S_i}^\beta \rangle = S(S+1)\left(\sum_j^\gamma {N_{ij}}^{\beta\gamma}\langle {S_j}^\gamma\rangle + \mu_B {g_i}^{\beta\alpha}H^\alpha\right)\Big/\left[3k_BT - S(S+1) \times \left(\sum_\gamma {B_i}^{\beta\gamma}{g_i}^{\gamma\alpha}/{g_i}^{\beta\alpha}\right)\right] + \text{order}\,(T^{-3}) \tag{4.1}$$

where

$${B_i}^{\beta\gamma} = (\tfrac{3}{5})\{1 + [(2 - 5\delta^{\beta\gamma})/4S(S+1)]\}{A_i}^{\beta\gamma}.$$

The factor in front of ${A_i}^{\beta\gamma}$ is 0.525 and 0.650 for the diagonal and off-diagonal elements

for Fe^{2+}, respectively, compared with 0.480 and 0.680 for Co^{2+}. Assuming self-consistency of the above equations, we find:

$$\langle S_i{}^{\beta} \rangle = C_i{}^{\beta\alpha} H^{\alpha}/(T - \theta_i{}^{\beta\alpha}) + \text{order}\,(T^{-3}) \tag{4.2}$$

where

$$C_i{}^{\beta\alpha} = [S(S+1)/3k_B] g_i{}^{\beta\alpha} \mu_B$$

$$\theta_i{}^{\beta\alpha} = [S(S+1)/3k_B] \left(\sum_{\gamma} B_i{}^{\beta\gamma} g_i{}^{\gamma\alpha} + \sum_{j\gamma} N_{ij}{}^{\beta\gamma} g_j{}^{\gamma\alpha} \right) / g_i{}^{\beta\alpha}.$$

Using the symmetry properties of the various parameters, we have transformed the above formulae to find the mean values of the spin modes $S_m{}^{\beta}$ which can be induced by H^{α}. These are the modes that belong to the group of the modes $F_m{}^{\alpha}$. The result is a simple change of i, j in (4.2) into m, n and the subtensor $\{N_{ij}{}^{\alpha\beta}\}$ becomes $\{N_{mn}{}^{\alpha\beta}(\Gamma)\}$. Through the tensor $\mathbf{g}$, every $\mathbf{S}$ mode yields a contribution to every $\boldsymbol{\mu}$ mode of the group. The magnetisation per ion induced by the field is given by the $\boldsymbol{\mu}$ modes $F_1{}^{\alpha}$ and $F_5{}^{\alpha}$. From the general relation

$$C_1/(T - \theta_1) + C_2/(T - \theta_2) = C/(T - \theta) + \text{order}\,(T^{-3}) \tag{4.3}$$

with

$$C = C_1 + C_2 \qquad C\theta = C_1\theta_1 + C_2\theta_2$$

comes

$$\langle \mu^{\alpha} \rangle = C^{\alpha} H^{\alpha}/(T - \theta^{\alpha}) = \chi_{\alpha} H^{\alpha} \tag{4.4}$$

where

$$C^{\alpha} = [S(S+1)/3k_B] \mu_B{}^2 \Gamma^{\alpha}$$

$$\theta^{\alpha}\Gamma^{\alpha} = [S(S+1)/3k_B](\tfrac{1}{2}) \sum_{m} \left(\sum_{\beta\gamma} g_m{}^{\alpha\beta} B_m{}^{\beta\gamma} g_m{}^{\gamma\alpha} + \sum_{n\beta\gamma} g_m{}^{\alpha\beta} N_{mn}{}^{\beta\gamma} g_n{}^{\gamma\alpha} \right)$$

$$\Gamma^{\alpha} = (\tfrac{1}{2}) \sum_{m\beta} g_m{}^{\alpha\beta} g_m{}^{\beta\alpha}.$$

Finally, when the field is applied along a direction $\boldsymbol{d}$ whose direction cosines are $\{R_{d\alpha}\}$ in $\boldsymbol{a}$, $\boldsymbol{b}$, $\boldsymbol{c}$, $\chi_d = R_{d\alpha}{}^2 \chi_{\alpha}$. Apart from χ_a, χ_b, χ_c no new information is available. This comes from the absence of the possibility that the component of $\mathbf{H}$ along one of the three axes gives rise to an $\mathbf{F}$ mode along another axis that is itself due to the orthorhombic symmetry of the crystal. From our measurements we obtain θ^{α} and Γ^{α} for $\boldsymbol{\alpha} = \boldsymbol{a}, \boldsymbol{b}$ and $\boldsymbol{c}$:

$$\theta^{\alpha} = \text{temperature to which } \langle \mu_{\alpha} \rangle^{-1}(T) \text{ extrapolates to zero} \tag{4.5}$$

$$\Gamma^{\alpha} = [4.5/S(S+1)]/[\text{slope of } \langle \mu_{\alpha} \rangle^{-1}(T) \text{ in the units of figure 3}].$$

These experimental values, deduced from the straight lines drawn in figure 3, are

Table 2. Quantitative information drawn from the susceptibility curves. From the observed paramagnetic susceptibility parameters Γ^α and θ^α, the combinations E1, E2 and E3 of the spin Hamiltonian parameters are deduced according to relations (4.6) and (4.8). Note that from the observed transition temperatures T_N, combinations E4 are deduced (see expressions (4.18), (4.19) and (4.22)).

A	α	Γ^α	θ^α	T_N	S	E1	E2	E3
Mn		4.00	−170	47.0	2.5	0	−58.3	~0
Fe	a	4.83	−103			0.21		−10.5
	b	5.13	−118	65.0	2	0.28	−46.0	−24.8
	c	4.35	−55			0.09		35.3
Co	a	6.03	−107			0.51		−80.6
	b	6.59	−19	50.0	1.5	0.65	−46.9	66.1
	c	6.31	−50			0.58		14.5

displayed in table 2. In (4.4), Γ^α is a quadratic expression of the tensor elements $g_m{}^{\alpha\beta}$. Defining by $\Sigma_\beta l_m{}^{\alpha\beta} S_m{}^\beta \mu_B$ the orbital contribution which, besides the spin contribution $2S_m{}^\alpha \mu_B$, contributes to the magnetic moment $\mu_m{}^\alpha$, then $g_m{}^{\alpha\beta} = 2\delta^{\alpha\beta} + l_m{}^{\alpha\beta}$, and

$$\Gamma^\alpha = 4 + 2\sum_m l_m{}^{\alpha\alpha} + (\tfrac{1}{2})\sum_{m\beta} (l_m{}^{\alpha\beta})^2 \tag{4.6}$$

or again

$$(\Gamma^\alpha - 4)/4 = (\tfrac{1}{2})\sum_m \left(l_m{}^{\alpha\alpha} + \sum_\beta (l_m{}^{\alpha\beta})^2 \right) = \mathrm{E1}.$$

This last expression is physically more explicit than the expression of Γ^α in (4.4) since it is the average over the two crystallographic sites of an expression that reduces to $l_m{}^{\alpha\alpha}$ in the limit $\mathbf{l}_m \ll 2$ (note that $l_5{}^{ab} = l_5{}^{bc} = 0$). The experimental values of E1 are shown in table 2. In (4.4) the various parameters of the model, $\mathbf{q}_m$, $\mathbf{A}_m$, J_{ij}, $\mathbf{T}_{ij}$, are combined to give θ^α. Looking for more explicit relations, that is, relations where the model parameters are less convoluted, it appears that this requires nothing less than regarding the $\mathbf{g}_m$ tensors as isotropic and equal at both sites. As a result of this approximation, one gets

$$3k_B\theta^\alpha/S(S+1) \simeq (B_1{}^{\alpha\alpha} + B_5{}^{\alpha\alpha})/2 + J_{12} + 2J_{57} + 2J_{15} + 4J_{35} + 4[U_{15}{}^{\alpha\alpha} + (U_{11}{}^{\alpha\alpha} + U_{55}{}^{\alpha\alpha})/2]. \tag{4.7}$$

The last term stands for the dipolar energy (assuming $\mathbf{g} = 2$). It amounts to about 40, 75 and −115 mK when $\boldsymbol{\alpha}$ is $\boldsymbol{a}$, $\boldsymbol{b}$ and $\boldsymbol{c}$, respectively, whatever the crystal. Thus, this term is negligible with respect to the left-hand term. The left-hand term can be considered as one of the three elements of a diagonal tensor, which is the average over all sites i of a tensor $\{\mathbf{B}_i{}^{\alpha\beta} + \Sigma_j J'_{ij}\delta^{\alpha\beta}\}$. Since $\mathbf{B}_i$ is traceless, this gives:

$$[1/S(S+1)] \sum_\alpha \theta^\alpha \simeq (1/k_B)(J_{12} + 2J_{57} + 2J_{15} + 4J_{35}) = \mathrm{E2} \tag{4.8}$$

and

$$[1/S(S+1)]\left(3\theta_\alpha - \sum_\beta \theta^\beta\right) \simeq (1/k_B)\,(B_1{}^{\alpha\alpha} + B_5{}^{\alpha\alpha})/2$$

i.e.,

$$\{20/3[4S(S+1)-3]\}\left(3\theta^{\alpha}-\sum_{\beta}\theta^{\beta}\right)\simeq(1/k_{B})(A_{1}{}^{\alpha\alpha}+A_{5}{}^{\alpha\alpha})/2=\mathrm{E3}.$$

The experimental values of E2 and E3 are shown in table 2. The parameters θ and Γ of the powder paramagnetic susceptibility are equal to $(\frac{1}{3})\Sigma_{\alpha}\theta_{\alpha}$ and $(\frac{1}{3})\Sigma_{\alpha}\Gamma^{\alpha}$, respectively, i.e., $-170, 4.00$ for A = Mn; $-92, 4.77$ for Fe, and $-58.7, 6.31$ for Co. They were -163, 3.93; -126, 6.06 and -65, 6.91, respectively, according to Nomura *et al* (1964) and Santoro *et al* (1966).

We have looked for analytical relations allowing the experimental parameters that define the paramagnetic susceptibilities to be linked to a restricted number of theoretical parameters. This led us to linearise the thermal average of the moments over the spin levels corresponding to the Hamiltonians (3.3). However, the validity of the corresponding relations (4.4) is bound to that of the assumptions that are necessary for this simplification. The theoretical parameters describing the spin levels of the lowest orbital level are here the tensors **A** and **g**. In the case of Fe_2SiO_4 and Co_2SiO_4, their link with the orbital levels of the orbital triplet $^5T_{2g}$ and $^4T_{1g}$, respectively, which constitutes the ground state of the ion in a cubic crystal field has been given by Ballet and Fuess (1989). Calling Δ the splitting between the two lowest orbital levels of this triplet, due to the non-cubic crystal field, and A^{ZZ}, A^{XX} the largest and weakest principal values of **A**,

$$A^{ZZ}-A^{XX}=2\rho^{2}\lambda^{2}/\Delta \tag{4.9}$$

and similarly, replacing A^{ZZ} by A^{YY}, and Δ by Δ', the splitting between the lowest and the highest orbital levels of the triplet. $\rho=-1$ for Fe^{2+} and $-\frac{3}{2}$ for Co^{2+}. This corresponds to the second-order effect of the spin–orbit coupling between the lowest orbital level and the two others. Within this approximation, $g^{XX}=2$, $g^{YY}=2(1-\rho\lambda/\Delta')$ and $g^{ZZ}=2(1-\rho^{2}\lambda/\Delta)$. However, (i) as $\rho^{2}\lambda/\Delta$ increases, the fourth-order effect yields an increasing anisotropy term of fourth order in the spins. (ii) The use of the spin Hamiltonian is itself limited by the condition $\Delta \gg k_{B}T$, which ensures that the levels not represented by the spin Hamiltonian are not populated. (iii) The linearisation of the thermal averages is justified as long as $k_{B}T$ is much greater than the greatest splitting in the spin levels issuing from the orbital ground state, i.e.,

$$k_{B}T \gg A^{ZZ}-A^{XX}. \tag{4.10}$$

(iv) Expression (4.4) neglects the so-called Van Vleck susceptibility. This contribution to the susceptibility is temperature-independent and comes from an orbital moment transfer from the two higher orbital levels to the low-lying one. This transfer does not depend on the spin states, and is induced by the coupling of the orbital levels by the magnetic field, via the term $-\mu_{B}\boldsymbol{H}\cdot\boldsymbol{L}$. For an ion, a field of 10 kOe applied along one of its principal axes A, induces a Van Vleck contribution of $(\frac{2}{3})(A^{AA}-A^{XX})/\lambda^{2}$ Bohr magneton. It is therefore maximum along the easy axis of magnetisation of the site, and increases with decreasing orbital splittings.

It has been shown by Ballet (1979) that the above constraints are more compelling than is often thought. In the simple case of an orbital doublet situated at 1500 K above the ground state, and with a spin–orbit constant $\lambda=-150$ K, $\chi^{-1}(T)$ was calculated by computer within the orbital triplet. The conclusions are as follows. If the resulting curves were observed experimentally, they could be fitted satisfactorily by straight lines. Because the inverse susceptibilities would not be very accurate above 250 K due to the weakness of the susceptibilities, this fit would be done in the range 100–250 K. However, these lines deviate significantly from those obtained analytically by linearisation of the thermal averages over the eigenstates of the second-order spin Hamiltonian. This is due

to the (iii) and (iv) effects described above. Effect (iii) shows itself as soon as a computer calculation of the thermal averages is performed within the orbital singlet. Below 200 K, the term of order T^{-2} is perceptible in $\chi(T)$ as well as that of order T^{-1} (i.e., the term of order T^0 beside that of order T in $\chi^{-1}(T)$) and the fitted lines extrapolate to lower θ^α than calculated analytically, especially along the axis of hard magnetisation. Effect (iv) appears when the two other orbital states are introduced into the computation. This actually transforms $\chi^{-1}(T)$ into $\chi^{-1}(T) - \chi^{VV} \times \chi^{-2}(T)$, which corresponds to a decrease in the slope of the fitted lines, increasing the apparent value of $\mathbf{g}$, especially along the axis of easy magnetisation.

In Mn_2SiO_4, there is no question of any low-lying excited orbital states and k_BT is always far greater than the elements of $\mathbf{A}_i$. Therefore, relation (4.4) is expected to be satisfactory. The observed susceptibility shows no significant anisotropy and a Curie law with $\mathbf{g} = 2$ fits well the thermal behaviour of the susceptibility above 100 K. The non-linearity of $\chi^{-1}(T)$ below this temperature is probably due to short-range order. The assumption leading to relation (4.8) from (4.4) is fully justified, and the E2 value reported in table 2 is expected to be good.

In Fe_2SiO_4, however, strong deviations from the above approximations are apparent. The succession of the axes that orders the Γ^α by increasing values, orders the θ^α by decreasing values. On the contrary, in a second-order spin Hamiltonian, the principal values of $\mathbf{g}$ and $\mathbf{A}$ are maximum along the same principal axes. Calculating by (4.9) the energy levels Δ and Δ' of an imaginary unique site whose principal axes would be $\boldsymbol{a}$, $\boldsymbol{b}$ and $\boldsymbol{c}$ along which the values would be those of our compound, gives 450 K and 2250 K if $\lambda = -130$ K. This shows that the lower excited orbital level of at least one of the two sites is probably not very high compared with $\rho\lambda$ and k_BT (hence (4.9) is not well justified). The model proposed in Ballet and Fuess (1989) to explain the magnetic structure observed in Fe_2SiO_4 and its thermal evolution was that at the 4a sites the highest principal value of $\mathbf{A}_i$ would be along a direction lying not far from the $\boldsymbol{c}$ axis, while at the 4c sites, it would be along $\boldsymbol{b}$. On account of the strength of the 4c anisotropy, which is needed to understand that the $\mathbf{G}$ modes are stabilised along the $\boldsymbol{b}$-direction despite the strong 4a anisotropy, the low θ^b value is puzzling. As for the high g^{bb} value, this could be due to a strong Van Vleck term in the 4c susceptibility. The fact that the susceptibility along $\boldsymbol{a}$ is not lower than that along $\boldsymbol{b}$ may be due to an M2 anisotropy favouring the $\boldsymbol{a}$-direction as well as the $\boldsymbol{b}$-direction. This is still compatible with a stabilisation of the Γ_{+++} magnetic group in spite of the M1 anisotropy which favours the $\mathbf{G}_1{}^c$ modes, i.e., the Γ_{+-+} group.

Other orders of magnitude are also interesting to deduce from the above picture of a unique site, which is the only means of making analytical estimates. A computation taking into account only the order 2 in λ/Δ would give the spin levels at 0, 1, 68, 88 and 104 K. The intensity of the fourth-order terms in S would be about $(\rho\lambda/\Delta)^2 \simeq 10\%$ of the intensity of those of second order. As for the magnetic entropy at T_N, it would be $k_B\ln(4.1) = 0.87k_B\ln(5)$ per ion. This could indicate that the discrepancy between the value $0.81k_B\ln(5)$ found by Robie *et al* (1982a) and $k_B\ln(5)$ is not necessarily due only to short-range order. The fourth-order terms are not expected to greatly modify the above spin level values, since our perturbation calculations to fourth order in the case of an axial anisotropy shows that the neglect of these terms leads to overestimating the minimum orbital splitting Δ, and to an insignificant change in the ratio between the maximum splitting of these spin levels and of the θ^a from which it has been deduced.

In Co_2SiO_4 the relative values of Γ^α, i.e., of $g_1{}^{\alpha\alpha} + g_5{}^{\alpha\alpha}$, are of the same order as the values of θ^α, i.e., of $A_1{}^{\alpha\alpha} + A_5{}^{\alpha\alpha}$. The maximum values correspond to $\boldsymbol{\alpha} = \boldsymbol{b}$, which is

the direction along which the moments develop their principal mode **G**. Here the picture of a unique site gives the energies at 1700 K and 2500 K if $\lambda = -230$ K, for the orbital levels, and at 0 and 130 K for the spin Kramers doublets. χ^{VV} is therefore weak, but the measurement temperatures are perhaps too low, especially along the ***a***-direction, to be sure that the term in $1/T^2$ is negligible in $\chi(T)$. The fourth-order contribution would be 4%. The magnetic entropy at T_N would be $k_B\ln(2.56) = 0.68k_B\ln(4)$ per ion. This is not far from the value of $0.71k_B\ln(4)$ per ion found by Robie *et al* (1982b). The excited doublet would be populated at 7% only at T_N, leading to an effective spin nearer to $\frac{1}{2}$ than to $\frac{3}{2}$ ($2S' + 1$ nearer to 2 than to 4) below T_N.

4.2. The ordering transition

The temperature for magnetic ordering is the highest temperature at which every spin can order under the action of the other spins. At the transition, the spins can be considered as small as necessary for the mean-field equations (3.2) to be linearised. We have found

$$\langle S_i{}^\alpha\rangle = S(S+1)\left(\sum_{j\beta}\langle S_j{}^\beta\rangle N_{ji}{}^{\beta\alpha}\right)\Big/\left[3k_BT - S(S+1)\right.$$
$$\left.\times\left(\sum_{j\beta}\langle S_j{}^\beta\rangle\sum_{k\gamma}N_{jk}{}^{\beta\gamma}B_k{}^{\gamma\alpha}\Big/\sum_{j\beta}\langle S_j{}^\beta\rangle N_{ji}{}^{\beta\alpha}\right)\right] + \text{order}\,(T^{-3}). \tag{4.11}$$

The transition requires self-consistency so that, replacing on the right of (4.11) $\langle S_i{}^\alpha\rangle$ by the expression (4.11), it becomes

$$\langle S_i{}^\alpha\rangle = S(S+1)\left(\sum_{j\beta}\langle S_j{}^\beta\rangle N_{ji}{}^{\beta\alpha}\right)\Big/\left[3k_BT - S(S+1)\right.$$
$$\left.\times\left(\sum_{k\gamma}\langle S_k{}^\gamma\rangle B_k{}^{\gamma\alpha}/\langle S_i{}^\alpha\rangle\right)\right] + \text{order}\,(T^{-3}). \tag{4.12}$$

Multiplying by the denominators, this becomes

$$\langle S_i{}^\alpha\rangle = [S(S+1)/3k_BT]\sum_{j\beta}(N_{ji}{}^{\beta\alpha} + B_j{}^{\beta\alpha}\delta_{ji})\langle S_j{}^\beta\rangle. \tag{4.13}$$

This requires that

$$\{N_{ij}{}^{\alpha\beta} + \delta_{ij}B_i{}^{\alpha\beta}\} = [3k_BT/S(S+1)]\{\text{unit tensor}\}. \tag{4.14}$$

The highest eigenvalue λ of the tensor on the left-hand side of (4.14) corresponds to the configuration with the highest transition temperature:

$$T_N = [S(S+1)/3k_B]\lambda. \tag{4.15}$$

The diagonalisation will be performed separately in the four subtensors $\{N_{mn}{}^{\alpha\beta}(\Gamma) + \delta_{mn}B_m{}^{\alpha\beta}\}$ expressed on the basis of the modes. Unfortunately, these subtensors are too large to allow an analytical expression of the eigenvalues to be found. However, with the assumption that the transition is governed by the projection of the tensor over the restricted basis ($G_1{}^\alpha$, $G_5{}^\alpha$) ($\boldsymbol{\alpha} = \boldsymbol{b}$ for Fe and Co, and $\boldsymbol{\alpha} = \boldsymbol{a}$ for Mn) this gives

$$\left(2J_{12} + \sum_{\beta\gamma} g_1{}^{\alpha\beta} U_{11}{}^{\beta\gamma} g_1{}^{\gamma\alpha} + B_1{}^{\alpha\alpha} - [3k_B T_N/S(S+1)]\right)$$
$$\times \left(-4J_{57} + \sum_{\beta\gamma} g_5{}^{\alpha\beta} U_{55}{}^{\beta\gamma} g_5{}^{\gamma\alpha} + B_5{}^{\alpha\alpha} - [3kT_N/S(S+1)]\right)$$
$$= \left(2J_{15} - 4J_{35} + \sum_{\beta\gamma} g_1{}^{\alpha\beta} U_{15}{}^{\beta\gamma} g_5{}^{\gamma\alpha}\right)^2. \tag{4.16}$$

Neglecting the energy of the dipolar interactions, we obtain

$$3k_B T_N/S(S+1) \simeq J_{12} - 2J_{57} + (B_1{}^{\alpha\alpha} + B_5{}^{\alpha\alpha})/2$$
$$+ \{[J_{12} + 2J_{57} + (B_1{}^{\alpha\alpha} - B_5{}^{\alpha\alpha})/2]^2 + [2J_{15} - 4J_{35}]^2\}^{1/2}. \tag{4.17}$$

For Mn_2SiO_4, we neglect the magnetocrystalline energy in front of the exchange energy, and we obtain

$$16.5\, k_B = J_{12} - 2J_{57} + [(J_{12} + 2J_{57})^2 + 4(J_{15} - 2J_{35})^2]^{1/2} = \text{E4 (Mn)}. \tag{4.18}$$

For Fe_2SiO_4, using the E3 value $(A_1{}^{\beta\beta} + A_5{}^{\beta\beta})$ of table 2, we obtain

$$32.3\, k_B = J_{12} - 2J_{57} + \{[J_{12} + 2J_{57} + 0.26\,(A_1{}^{bb} - A_5{}^{bb})]^2$$
$$+ 4(J_{15} - 2J_{35})^2\}^{1/2} = \text{E4 (Fe)}. \tag{4.19}$$

However, as seen in the preceding section, at the transition all the spin levels are probably not populated, at least on one site. Moreover, the necessary reduction of the tensor to the above-mentioned projection may be not a good approximation because of the high $A_1{}^{bc}$ value that is responsible for the canting of the 4a moments, which appears below the transition.

For Co_2SiO_4, it was shown in § 4.1 that the assumptions on which the calculation leading to (4.17) is based, do not hold. Actually, at T_N the higher spin doublet is barely populated, and the behaviour of the Co^{2+} ions is led by the lower spin doublet ($S' = \frac{1}{2}$). Taking only this doublet into account, a calculation of the mean field T_N value can be performed in the following way.

The eigenstates of the spin Hamiltonian in a site i can be described by

$$\begin{aligned} &\gamma|\tfrac{3}{2}\rangle + \delta|-\tfrac{1}{2}\rangle \quad \text{and } \gamma|-\tfrac{3}{2}\rangle + \delta|\tfrac{1}{2}\rangle, \quad \text{at } -(\tfrac{3}{4})A_i{}^{bb}x_i \\ &\delta|\tfrac{3}{2}\rangle - \gamma|-\tfrac{1}{2}\rangle \quad \text{and } \delta|-\tfrac{3}{2}\rangle - \gamma|\tfrac{1}{2}\rangle, \quad \text{at } +(\tfrac{3}{4})A_i{}^{bb}x_i \end{aligned} \tag{4.20}$$

where $x_i^2 = 1 + \eta^2/3$, $\eta = (A_i{}^{cc} - A_i{}^{aa})/A_i{}^{bb}$, $\gamma^2 = (x_i + 1)/2x_i$ and $\delta^2 = (x_i - 1)/2x_i$. (The quantum problem is formally equivalent to the hyperfine interaction of an electric field gradient acting on the $I = \frac{3}{2}$ state of a Mössbauer nucleus ^{57}Fe.) With $A_i{}^{bb} > 0$, the fundamental doublet is the first one. Within this doublet, the term $-\Sigma_{n\alpha} N_{mn}{}^{b\alpha} \langle S_n{}^{\alpha}\rangle S_m{}^{b}$ is diagonal and generates a splitting equal to $(3\gamma^2 - \delta^2)\Sigma_{n\alpha} N_{mn}{}^{b\alpha}\langle S_n{}^{\alpha}\rangle$. At the transition, the splitting is vanishingly small. Therefore it is very small with respect to $k_B T$. Along $\boldsymbol{b}$, the spin quantum mean is ξ_m (or $-\xi_m$) on the ground (or excited) level. Its thermal average is

$$\langle S_m{}^{b}\rangle = (1/k_B T)\xi_m{}^2 \sum_{n\alpha} N_{mn}{}^{b\alpha}\langle S_n{}^{\alpha}\rangle, \qquad \text{with } \xi_m = (x_m + 2)/(2x_m). \tag{4.21}$$

The transition arises when consistency is reached, i.e., when $k_B T$ is small enough to be

an eigenvalue of the tensor $\{\xi_m{}^2 N_{mn}{}^{\alpha\beta}\}$. Considering only the projection over $\{G_1{}^b, G_5{}^b\}$, which is justified since the canting is weak, one gets:

$$k_B T_N = 49.3\, k_B \simeq \xi_1{}^2 J_{12} - 2\xi_5{}^2 J_{57} + [(\xi_1{}^2 J_{12} + 2\xi_5{}^2 J_{57})^2 + 4\xi_1 \xi_5 (J_{15} - 2J_{35})^2]^{1/2} = \text{E4 (Co)}. \tag{4.22}$$

Note that in the particular case $\xi_1 = \xi_5 = \xi$, this gives $k_B T_N = \xi^2 \times$ {right-hand term of formula (4.18)}. For $A_m{}^{cc} = A_m{}^{aa} = (-\frac{1}{2}) A_m{}^{bb}$, $\xi^2 = 2.25$, while for $A_m{}^{cc} = A_m{}^{bb} = (-\frac{1}{2}) A_m{}^{aa}$, $\xi^2 = 1.0$. This shows clearly the great effect of single-ion anisotropy on T_N.

In contrast with the θ^α values, which are determined by the susceptibility at temperatures where the mean-field approximation is satisfactory, the T_N value is sensitive to short-range correlations. Their effect is to decrease the T_N value from the mean-field value by retaining the paramagnetic state, so that the E4 values above may be underestimated. This effect is more important for weaker anisotropy (de Jongh and Miedema 1974), hence it is expected to be the most important in Mn_2SiO_4 (Heisenberg three-dimensional magnet) and the least in Co_2SiO_4 (Ising-type three-dimensional magnet).

4.3. Below T_N

Now we discuss qualitatively the evolution of the magnetisation induced under 10 kOe, in the three crystals, along the axes ***a***, ***b*** and ***c***. Since any macroscopic magnetisation along a direction ***α*** is due to the $F_m{}^\alpha$ modes, this reduces to studying these modes when a field $H = H^\alpha$ is applied and when the temperature varies. However, the intensity of these modes never exceeds 0.08 μ_B per ion when $H = 10$ kOe, while the intensity of the **G** modes is in the range 3–5 μ_B per ion. Moreover, the interactions responsible for the zero-field magnetic structure are far greater than the interaction of the spins with ***H***. Therefore, the main modes will always be those that constitute the zero-field structure. It is worthwhile remembering the following classical result on the collinear antiferromagnets with only one class of magnetic sites. If an anisotropy precludes a rotation of the moments, a field applied along them gives rise to a susceptibility decreasing to zero when T decreases from T_N to 0 K ($\chi_\parallel$). When the field is perpendicular to the moments, the susceptibility stays nearly constant ($\chi_\perp$).

In Mn_2SiO_4, the difference $M_c - M_b$ below 47.7 K is exactly the remnant magnetisation appearing in the $M_c(H)$ curves. It is also found as $M_c(T)$ measured in a weak field just large enough to preclude the building of the weak ferromagnetic domains (figure 2, insert). Therefore, the initial susceptibilities χ_c and χ_b are equal. χ_a is only a little smaller. Along the three directions the susceptibility has a $\chi_\perp$ character. Along ***b*** and ***c*** this is normal since the zero-field configuration is along ***a***. The decrease in χ_a just below T_N, where the moments of the 4a sites are small with respect to those on the 4c sites (see Ballet and Fuess 1989), may correspond to a $\chi_\parallel$ character of the susceptibility of the 4c moments, which are aligned along ***a***. Because χ_a does not decrease further when the temperature continues to fall, a field-induced rotation of the configuration seems to be necessary to explain it. However, a magnetocrystalline anisotropy is required to explain why the axis ***a*** is chosen for the **G** modes, since the dipolar energy does not favour this direction (Ballet and Fuess 1989). The energy saved by a rotation would be less than 25 mK (taking into account the M1 canting), so it is unlikely that the rotation would happen. Consequently, we think that at low temperatures, χ_a is due mainly to the components on the 4a sites perpendicular to the ***a***-axis. The weak ferromagnetism results

from a small canting of the moments towards the ***c*** direction. Within the Γ_{--+} symmetry group, such canting actually gives rise to the $F_m{}^c$ modes. The canting may result from an anisotropic exchange coupling, or from the dipolar interactions, as well as from a weak single-ion anisotropy. The decrease of the weak ferromagnetism below 14 K may be correlated with the onset of the $A_1{}^b$ mode which spoils the $G_1{}^a$ mode a part of its length. This assumption requires that a part of the weak ferromagnetism is due to an $F_1{}^c$ mode created by the action of a non-zero anisotropy term $A_1{}^{ca}$ on the $G_1{}^a$ mode.

In Fe_2SiO_4, the susceptibility along ***b*** decreases below T_N, while along ***a*** it increases very slowly. This is understandable in view of the antiferromagnetic structure which is mainly along ***b***. However, a remarkable feature of the susceptibility curves is the absence of any accident on χ_c at T_N. The susceptibility continues to increase when T decreases below T_N. The Curie law is still followed until, at 20 K, χ_c begins to fall. We think that this pseudo-paramagnetic behaviour is due to the 4a sites. The antiferromagnetic order sets up mainly in the 4c planes. The 4a spins bridge these planes. The 4a spins are submitted to two contradictory forces. One of them is internal to the ion, and it attracts the spins toward a direction which is near the ***c***-axis. The other arises from the exchanges with the 4c spins (J_{15}–$2J_{35}$) necessary for the magnetic order that appears at T_N. It attracts the spin along the 4c magnetic structure, i.e., along ***b***. The 4a–4a exchange coupling (J_{12}) should be weak. This, added to the above conflict, gives to the 4a spins a great susceptibility to the action of an external field, and especially along ***c***. The very slow saturation of the 4a moments when T decreases, and the single-ion anisotropy of the 4a sites which was required to explain the thermal behaviour of the canting (Ballet and Fuess 1989) are quite consistent with this view. The fall of χ_c below 20 K results from the increase of the canting: when the moments come closer to the ***c***-direction and are better ordered, χ_c adopts some $\chi_\parallel$ character.

In Co_2SiO_4, the general trend of the susceptibility is more common than in Fe_2SiO_4. χ_b has a strong $\chi_\parallel$ character, while χ_c and χ_a are $\chi_\perp$-like. This is in agreement with the main direction of the moments which is ***b***. The ***c***-direction is favoured, compared with the ***a***-direction. But it is not possible to know how this anisotropy is distributed between the two classes of sites. The non-zero value of χ_b at $T = 0$ K is probably due to the canting of the 4a moments, which introduces some $\chi_\perp$ character in χ_b. Similarly, some $\chi_\parallel$ character of the susceptibilities along ***c*** and ***a***, which do not decrease down to 0 K, are probably responsible for their slight decrease below T_N.

5. Conclusion

The realisation of single crystals has allowed the measurement of the anisotropy of the magnetic susceptibilities of Mn_2SiO_4, Fe_2SiO_4 and Co_2SiO_4. The strong anisotropy detected in Fe_2SiO_4 and Co_2SiO_4 confirms the assumption made by Ballet and Fuess (1989) that the thermal behaviour of their magnetic structure is strongly determined by their magnetocrystalline anisotropies. The weak ferromagnetism measured along the ***c***-axis of Mn_2SiO_4 could be predicted from the observed magnetic structure by the magnetic symmetry group approach, and hence confirms the validity of this approach. The special thermal behaviour of the susceptibility observed along the ***c***-axis in Fe_2SiO_4 seems to be in good agreement with the view proposed by Ballet and Fuess (1989) to explain the thermal evolution of the canting of the M1 moments in this compound. That is to say, the M1 ions thermodynamics is dominated by the competition between their strong

single-ion anisotropy favouring a direction near the *c*-axis, and their exchange interactions with the M2 moments attracting them along the *b*-direction.

The susceptibility observed in Co_2SiO_4 is in good agreement with the observed magnetic structure. The establishment of analytical relations between the experimental parameters drawn from the magnetisation curves, C^{α}, θ^{α}, T_N, and temperature-independent theoretical parameters describing the electronic state of the ions and their interactions, was pushed as far as possible. On the one hand, these analytical relations require that, in particular, the ion can be modelled by a second-order spin Hamiltonian. On the other hand, the existence of two types of fourfold sites, leads to an important underdetermination of the theoretical parameters. The microscopic susceptibility tensors are not observed, and one is led to consider an intermediary picture: that of a macroscopic or mean site defined as one that would have a susceptibility tensor equal to the observed macroscopic one.

Using the relationship between the spin Hamiltonian parameters and orbital levels, it has been shown that the parameters deduced from the experiments through the analytical relations correspond to orbital levels that do not always fulfil the conditions required to justify the representation of the sites by a second-order spin Hamiltonian, and hence to justify the analytical relations themselves. However, for Fe_2SiO_4 and Co_2SiO_4 the magnetic entropy calculated at T_N by considering the level scheme of the above-defined mean site does not disagree with that determined by Robie *et al* from specific heat measurements.

The ensemble of the experiments performed on Mn_2SiO_4, Fe_2SiO_4 and Co_2SiO_4 by neutron diffraction and magnetic measurements, has allowed us to establish a model that is consistent with the main features of the observed magnetic behaviour in all three compounds. Computer simulations (Ballet and Fuess, to be published) of the magnetic structures, susceptibilities and specific heats, which require fewer approximations than the analytical approach, and are not confined to a choice of a small number of experimental parameters, confirm the main trends of this model.

Acknowledgments

Support of this work by the Bundesminister für Forschung und Technologie is gratefully acknowledged.

References

Ballet O 1979 *Thesis*, University of Grenoble
Ballet O and Fuess H 1989 *J. Phys. Chem. Solids* at press
Bertaut E F 1963 *Treatise on Magnetism* vol 3, ed. G T Rado and H Suhl (New York: Academic Press) pp 149–209
de Jongh L J and Miedema A R 1974 *Adv. Phys.* **23** 1–260
Foner S 1959 *Rev. Sci. Instrum.* **30** 548–57
Lottermoser W and Fuess H 1988 *Phys. Stat. Solidi* (a) **109** 589–95
Lottermoser W, Müller R and Fuess H 1986 *J. Mag. Magn. Mater.* **54–57** 1005–6
Müller R, Fuess H and Brown P J 1982 *J. Physique* **C7** 249–52
Nomura S, Santoro R, Fang J and Newnham R 1964 *J. Phys. Chem. Solids* **25** 901–5
Robie R A, Finch C B and Hemingway B S 1982a *Am. Miner.* **67** 463–9
Robie R A, Hemingway B S and Takei H 1982b *Am. Miner.* **67** 470–82
Santoro R P, Newnham R E and Nomura S 1966 *J. Phys. Chem. Solids* **27** 655–66

Takei H and Hosoya S 1982 *Adv. Earth Planetary Sci.* **12** 537–47
Takei H, Hosoya S and Ozima M 1984 *Materials Science of the Earth's Interior* ed. I Sunagawa (Tokyo: Terrapub) pp 107–30